

## Ortho-para dependence of the equation of state and the phonon frequency of solid hydrogen

A. Driessen\*

*Natuurkundig Laboratorium Universiteit van Amsterdam, Valckenierstraat 65, 1018 XE Amsterdam, The Netherlands*

Isaac F. Silvera

*Lyman Laboratory of Physics, Harvard University, Cambridge, Massachusetts 02138*

(Received 1 December 1986)

The influence of the rotational state on the equation of state and the phonon frequency of solid molecular hydrogen has been studied experimentally under isochoric conditions at several densities. An analysis of the equation-of-state data has made it possible to separate the contributions from the isotropic and the anisotropic part of the interaction potential. In this way a previous model for the calculation of the anisotropic contribution, mainly of an electric quadrupole nature, could be confirmed. The change of the isotropic potential is given in terms of the parameters of the interaction potential due to Silvera and Goldman. Finally, a short analysis of the experimentally determined changes in phonon frequency is given.

### I. INTRODUCTION

Solid molecular hydrogen is a very soft compressible material at low pressures and undergoes large volume changes with modest changes in pressure. The equation of state (EOS) of  $H_2$  is determined by the intermolecular potential which has a large isotropic part and a weak anisotropic part at low pressures. Although the EOS is dominated by the isotropic part, at low temperatures the anisotropic interactions give rise to interesting and easily measurable modifications to the EOS. A great advantage for studying these effects is afforded by the existence of ortho and para molecules (ortho corresponds to odd rotational states designated by the quantum number  $J$ ; para to even rotational states).<sup>1,2</sup> At low temperatures, to a good approximation, the molecules are in free-rotor single molecular states and only the para  $J=0$  and ortho  $J=1$  rotational states are populated because of the large splitting of several hundred degrees K of the rotational levels [ $E=BJ(J+1)$ , with  $B \approx 85.4$  K]. Since the single-molecule wave functions are spherical harmonics, the  $J=0$  state is spherically symmetric while the  $J=1$  state is anisotropic. As a consequence, at low pressure, interactions between para molecules are isotropic, while ortho molecules interact both isotropically and anisotropically [mainly through the electric quadrupole-quadrupole (EQQ) interaction]. Thus pure  $p$ - $H_2$  does not have anisotropic interactions and effects of anisotropic interactions on the EOS will depend on the ortho concentration,  $C_1$ . For example, an isochoric sample of  $o$ - $H_2$  will have a sharp drop in pressure when it has a transition from an hcp structure into the orientationally ordered  $Pa3$  structure at a few degrees K as the crystal energy due to the EQQ interaction is lower for smaller intermolecular separations; no such effect occurs in solid  $p$ - $H_2$  which remains hcp to  $T=0$  K. For  $C_1 \lesssim 0.55$  the phase transition does not occur, but the pressure gradually falls as the temperature is lowered, again due to the EQQ interaction.

In general, an  $H_2$  sample will not have a thermodynam-

ic equilibrium mixture of ortho and para (in thermodynamic equilibrium  $C_1=0$  for  $T=0$  K and  $C_1=0.75$  for  $T=300$  K). This is a result of the forbidden nature of the  $o$ - $p$  transition, so that conversion rates are of the order of a few percent per hour.<sup>3</sup> This affords a very interesting way for sorting out the effects of anisotropic interactions on the EOS. An isochoric sample can be studied for several days as  $C_1$  slowly changes from a high value towards zero. This is what we have done.

In this article we study the effect of ortho concentration on the EOS. The main effect due to anisotropic interactions was first observed by Jarvis *et al.*<sup>4</sup> at low pressures, to  $P \approx 100$  bars. This is the temperature-dependent effect already mentioned due to the short-range ordering of the molecules to reduce the potential energy due to the EQQ interaction. Later, Driessen *et al.*<sup>5</sup> gave an expression for the calculation of the so-called quadrupolar pressure,  $P_Q$ , as a function of  $C_1$ , volume, and temperature. Here we look beyond this effect and find a very subtle effect depending on the  $C_1$  concentration. Due to the centripetal force, an ortho molecule has a larger molecular diameter than a para. As a consequence, the isotropic interaction for ortho molecules interacting with their environment changes. We have been able to determine this dependence on  $C_1$ .

In the following section the theoretical basis for interpreting the EOS data as well as phonon frequencies, which we have also studied, is given in terms of the parameters of the pair potential. The experimental system is discussed in Sec. III, followed by a discussion and comparison to theory and some conclusions.

### II. THEORETICAL BACKGROUND

In this section we establish a connection between the EOS of solid molecular hydrogen and the parameters of the pair interaction potential.<sup>1,2</sup> We also include a brief discussion of the dependence of the phonon frequency on  $C_1$ .

The interaction between two molecules is a complex function of the intermolecular separation  $R$  and the orientation of the two molecules,  $\Omega_1$  and  $\Omega_2$ . To a good approximation one can separate the potential  $V_P$  into an isotropic part,  $V_I$  and an anisotropic part,  $V_A$ ,

$$V_P(R, \Omega_1, \Omega_2) = V_I(R) + V_A(R, \Omega_1, \Omega_2). \quad (1)$$

$V_A$  has the property that it is zero for a pair of spherically symmetric  $J=0$  molecules. This is of special interest for the experimentalist, who can vary the effect of the anisotropic interaction simply by choosing the desired concentration of  $J=1$  molecules. At low density,  $V_A$  is mainly due to the electric quadrupole moment and has a nonzero value for a pair of  $J=1$  molecules. We shall neglect other contributions, which are at least one order of magnitude smaller.

The electric quadrupole-quadrupole interaction term included in  $V_A$  can be written as  $V_Q = \Gamma \times$  (geometrical factor), where one can write

$$\Gamma = 6e^2 Q^2 / 25R^5. \quad (2)$$

Here,  $Q$  is the electric quadrupole moment. For solid  $H_2$  at zero pressure,  $\Gamma \equiv \Gamma_0 = 0.95$  K. This potential is responsible for a splitting of  $10\Gamma$  of the energy depending on the relative orientation of the two molecules as shown in Fig. 1. The ground state at an energy of  $-4\Gamma$  corresponds to a classical  $T$  orientation in which the molecular axes are perpendicular to each other. In Fig. 1 we see that other interactions have only a small effect on the energetics.

One of the important effects that we shall study is the difference in  $V_I$  for para and ortho molecules due to the different molecular diameters of the two species. Knaap and Beenakker<sup>6</sup> made the following ansatz for the centripetal expansion

$$K(h_1 - h_0) = mh_0\omega^2 = \frac{2\hbar^2}{Ih_0} = 4k_B\Theta_{\text{rot}}/h_0, \quad (3)$$

where  $\omega$  is the rotational frequency, and  $h_0$  and  $h_1$  are the bond lengths in the hydrogen molecule for the  $J=0$  and

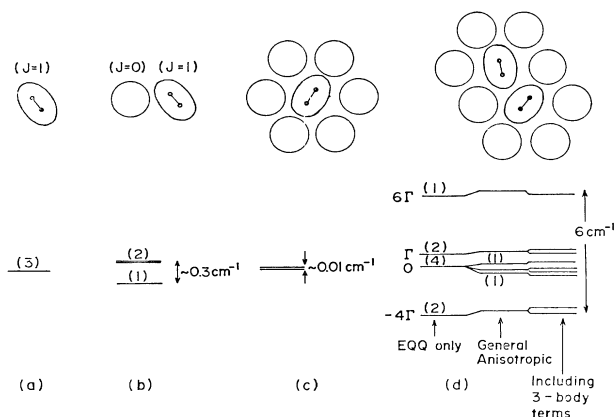


FIG. 1. The energy levels of a  $J=1$   $H_2$  molecule in different environments for the zero pressure solid: (a) isolated ortho molecule, (b) an ortho-para pair, (c) ortho molecule in a  $p$ - $H_2$  lattice, (d) an  $o$ - $H_2$  pair in a  $p$ - $H_2$  lattice.

$J=1$  species;  $K$  the restoring force constant has a value  $570 \text{ J m}^{-2}$ ,  $h_0 = 74 \times 10^{-12} \text{ m}$ , and  $\Theta_{\text{rot}} = 85.4 \text{ K}$ . The resulting difference in bond length is

$$h_1 - h_0 = 0.112 \times 10^{-12} \text{ m}. \quad (4)$$

In their paper, Knaap and Beenakker study the effect of this change in bond length on the repulsive and attractive pair potential. They use a Lennard-Jones (LJ) potential and give the resulting shift in the well depth,  $\Delta\epsilon$ , and hard-core parameter,  $\Delta\sigma$ , for hydrogen. We expect these results only to be indicative of the order of magnitude, because the LJ potential has proven to be inadequate for generating the EOS of hydrogen. We therefore prefer to use the semiempirical potential due to Silvera and Goldman<sup>7</sup> which we shall designate as the SG potential.

We consider the attractive and repulsive parts separately. The attractive part is given as

$$V_{\text{SG attr}} = \sum_{i=6,8,10} C_i / R^i, \quad (5)$$

where  $R$  is the intermolecular distance. The constants  $C_i$  are taken from Meyer.<sup>8</sup> Fortunately Meyer gives the  $C_i$ 's for different bond lengths, because he considers the intramolecular vibrational average of the  $C_i$ 's.

We make a linear interpolation of Meyer's values for two different bond lengths in order to obtain  $\Delta C_i = C_i(h_1 - h_0)$ ,

$$\Delta C_i = \frac{C_i(\langle h \rangle) - C_i(h_e)}{\langle h \rangle - h_e} (h_1 - h_0). \quad (6)$$

$h_e = 1.40$  a.u.;  $\langle h \rangle = 1.449$  a.u. In Table I we provide the calculated  $C_i$ 's of Meyer and our interpolated ones.

*Ab initio* calculations also exist for various bond lengths for the repulsive part of the potential (McMahan *et al.*,<sup>9</sup> Ree and Bender,<sup>10</sup> and Min *et al.*<sup>11</sup>). The problem of expressing the influence of the change in the bond length on the parameters of the SG potential are more serious than with the attractive part. Ree and Bender<sup>10</sup> have calculated  $V_{\text{rep}}$  at various intermolecular distances (from 2 to 5 a.u.) and various bond lengths. They found the expected minimum for  $V_{\text{rep}}$  at a bond length of about 1.4 a.u. With a known change in bond length, it should be possible to determine the change in  $V_{\text{rep}}$ . Figure 2, taken from Ref. 12, displays  $V_{\text{rep}}$  qualitatively as a function of the bond length,  $h$ . Also the probability distribution of the intramolecular separation in a given quantum state is shown. Even in the ground state,  $V_{\text{rep}}$  changes nearly an order of magnitude within the half width of this distribution. Therefore only a detailed calculation involving the distribution function of the intramolecular vibration and a

TABLE I. The  $C_i$ 's as calculated by Meyer (Ref. 8) and  $\Delta C_i = C_i(h_1) - C_i(h_0)$ ; all values in a.u.

	$h = h_e$	$h = \langle h \rangle$	$\Delta C_i$
$C_6$	11.4	12.12	0.0323
$C_8$	196.7	213.3	0.7453
$C_{10}$	4303.0	4741.0	19.66

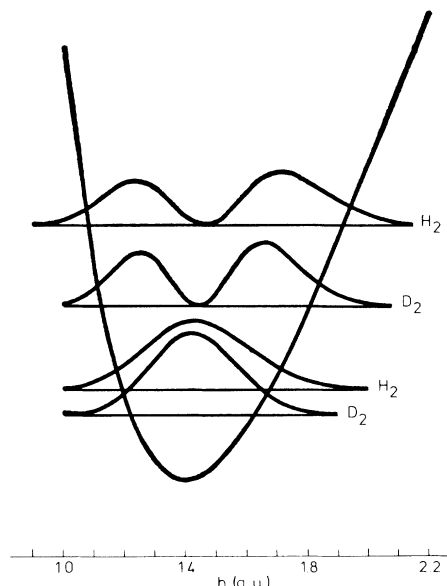


FIG. 2. The probability distribution of the intermolecular separation  $h$  in the ground and first excited states.  $V_{\text{rep}}$  as a function of  $h$  (a.u.) is also shown qualitatively.

detailed knowledge of the asymmetric  $V_{\text{rep}}$  can provide a  $\Delta V_{\text{rep}}$  with satisfactory accuracy.

We made several crude approximations for this calculation. These only enabled us to give some extreme bounds for  $\Delta V_{\text{rep}}$ . The repulsive part of the SG potential

$$V_{\text{SGrep}} = e^{\alpha - \beta R - \gamma R^2}, \quad (7)$$

with  $\alpha = 1.713$ ,  $\beta = 1.5671$ , and  $\gamma = 0.00993$ , reproduces the numerical results of Ree and Bender fairly well for 2 a.u.  $< R < 5$  a.u. When we now fit a  $\Delta\alpha = \alpha(h_1) - \alpha(h_0)$  of Eq. (7) as a parameter to account for the  $\Delta V_{\text{rep}}$  from the above calculation, we get  $2 \times 10^{-4} < \Delta\alpha < 5 \times 10^{-2}$ . The boundaries reflect the large scatter in the *a priori* determination of  $\Delta V_{\text{rep}}$ . As stated above, only more detailed calculation can give meaningful results. We have not done these calculations. Instead, in Sec. V we determine  $\Delta\alpha = 3.4 \times 10^{-3}$ , which lies inside the scatter of the *a priori* results.

As our experimental data consist mainly of EOS measurements, we would like to analyze the effect of  $C_1$  on pressure. A way of doing this is to use the pair potential to calculate the free energy  $F(V, T, C_1)$  of the solid. Using the thermodynamic relation

$$P(V, T, C_1) = - \left[ \frac{\partial F(V, T, C_1)}{\partial V} \right]_T \quad (8)$$

it is possible to calculate the pressure. Similar to the splitting of the pair potential in an isotropic and anisotropic part we write, to a good approximation,

$$F(V, T, C_1) = F_I(V, T, C_1) + F_A(V, T, C_1). \quad (9)$$

With Eq. (8) we get analogous expressions for the pressure

$$P(V, T, C_1) = P_I(V, T, C_1) + P_A(V, T, C_1). \quad (10)$$

$P_I(V, T, C_1)$  is essentially the lattice contribution to the pressure  $P_L(V, T, C_1)$ ; whereas  $P_A(V, T, C_1)$  is mainly given by the quadrupolar pressure  $P_Q(V, T, C_1)$ .

Concentrating first on the lattice pressure, we can separate this into a zero-temperature and thermal pressure part,

$$P_L(V, T, C_1) = P_{OL}(V, C_1) + P_L^*(V, T, C_1). \quad (11)$$

We can also partition this for the  $C_1$  dependence

$$P_L(V, T, C_1) = P_{OL}(V) + P_{IL}(V, C_1) + P_L^*(T, V) + P_{IL}^*(T, V, C_1). \quad (12)$$

The term  $P_{OL}(V)$  is the  $T=0$  isotherm for para- $\text{H}_2$ , and  $P_L^*(T, V)$  the phonon induced thermal pressure of *p*- $\text{H}_2$ . Both are given in dense tabulation in Ref. 13. The two other contributions in Eq. (12) are due to the change in the intramolecular distance of the  $\text{H}_2$  molecule. From spectroscopic data it is known that the rotational constant  $B$  does not change within the temperature region of our experiment. With Eq. (3) this implies that the intramolecular distance also will not change with temperature. Therefore  $P_{IL}$ , which represents the ortho-para-dependent part of the isotropic potential, and which we have experimentally determined as one of the principal objectives of this work is expected to be small and will be neglected in the following paragraph.  $P_{IL}$  will actually be determined by subtracting off the calculated quadrupolar pressure from the isochoric pressure measured as a function of ortho concentration.

For the quadrupolar pressure  $P_Q(V, T, C_1)$  in a previous work<sup>5</sup> we derived an expression based on a model for the quadrupolar specific heat by Berlinsky and Harris.<sup>14</sup> For

TABLE II. Values of  $-P_Q V/T$  determined by evaluating Eq. (13) as a function of  $G(V, T, C_1) = 154 V^{-5/3}/T$  for selected values of  $C_1$ . ( $P_Q$  is given in bars,  $V$  in  $\text{cm}^3/\text{mole}$ , and  $T$  in kelvin.)

$G$	$C_1$				
	0.2	0.4	0.6	0.8	1.0
0.01	0.03	0.10	0.23	0.41	0.63
0.02	0.10	0.40	0.90	1.59	2.48
0.03	0.23	0.89	1.99	3.50	5.41
0.04	0.40	1.56	3.46	6.05	9.30
0.06	0.87	3.38	7.39	12.8	19.4
0.08	1.50	5.75	12.4	21.1	31.6
0.10	2.28	8.57	18.2	30.5	45.1
0.15	4.71	17.0	34.6	56.2	80.7
0.20	7.67	26.4	52.3	82.6	115.8
0.30	14.5	46.5	87.5	133.0	180.1
0.40	21.8	66.5	121.0	179.1	
0.60	36.9	105.0	182.5		
0.80	52.0	141.2			
1.00	66.9	175.4			

the quadrupolar pressure one finds

$$P_Q(V, T, C_1) = -\left(\frac{5}{3}\right)V \int_{x=T}^{\infty} C_{VQ}(V, x, C_1) dx . \quad (13)$$

The quadrupolar specific heat  $C_{VQ}$  is always positive, therefore  $P_Q(V, T, C_1)$  is always a negative pressure. The set of parameters and functions needed for the evaluation of Eq. (13) is given in Ref. 5. The results of this calculation is conveniently given as  $P_Q V/T$  versus the dimensionless parameter  $\Gamma/T$ , where

$$\Gamma_{H_2}(V) = \Gamma_{D_2}(V) = 154V^{-5/3} , \quad (14)$$

$$\Delta\omega_{\text{tot}}(V, T)/\omega(V, T) = \frac{1}{\omega(V, T)} \{[\omega_{IL}(V) + \omega_Q(V, T)] + [\Delta\omega_{\text{tot}}(V, T)/\Delta P][P_Q(V, T) + P_{IL}(V)]\} , \quad (15)$$

where

$$\Delta\omega_{\text{tot}}(V, T) = \omega(C_1 = 1, V, T) - \omega(C_1 = 0, V, T) ,$$

$\omega_{IL}(V)$  is the frequency change due to the change in the isotropic potential and  $\omega$  is the frequency of the  $p$ -H<sub>2</sub> optical phonon. The term  $\omega_Q(V, T)$  is the result of a change in the anisotropic EQQ interaction. This quantity is small; even in the ordered state it is less than  $5 \times 10^{-3}\omega$ . The last term takes account of pressure changes at constant volume, which also cause a frequency shift. It will be shown in the last section that this is the leading term.

In Eqs. (5) and (7) we introduced the SG potential for  $p$ -H<sub>2</sub>. In the original work<sup>7</sup> an effective interaction potential for the solid is given from which the free energy of  $p$ -H<sub>2</sub> and  $o$ -D<sub>2</sub> could be calculated in the self-consistent phonon approximation for an fcc lattice. With use of Eq. (8) the  $T=0$  isotherm,  $P_{OL}(V)$  for  $p$ -H<sub>2</sub> was derived, in good agreement with experiment. We used these computer codes<sup>16</sup> to calculate the partial derivatives of the pressure with respect to small changes in the parameters. Having once found new parameters for the  $C_1=1$  isotropic potential (see Sec. V) we are able to calculate  $P_{ILSG}(V)$ .

### III. EXPERIMENTAL SETUP

To determine  $P_{IL}(V, T, C_1)$  we measured the pressure on an isochore as a function of temperature and concentration  $C_1$  at several different volumes. The condition that for a certain run all data points should be taken on an isochore, i.e., at constant volume, was easy to obtain, because the concentration  $C_1$  of H<sub>2</sub> changes as a function of time when the solid is out of rotational equilibrium. This conversion is slow enough to enable measurements of isochores characteristic of a given concentration, but quick enough to provide significantly large changes within a reasonable time ( $\sim 100$  h).

For the experiments, we started with samples of normal-H<sub>2</sub> (75%  $o$ -H<sub>2</sub>), which converted slowly to about 20% in the course of the measurement. The change of  $C_1$  was large enough to measure the effects with reasonable precision. The experiments were done in an isochore cell,

with  $V$  in cm<sup>3</sup>/mole and  $\Gamma$  in kelvin. In Eq. (14) we use the experimental  $\Gamma(V)$  instead of the rigid lattice value  $\Gamma_0(V)$  [Eq. (2)], which is reduced by the zero-point motion and charge overlap. In Table II a sufficient number of points is given to enable easy interpolation. (In our previous work<sup>5</sup> we presented a similar table, which however contained a numerical error<sup>15</sup>).

In our measurements we have also determined the frequency of the Raman active optical phonon as a function of temperature and  $C_1$  at different densities. To interpret these data we separate the different contributions to the frequency shift analogous to the different pressure contributions [see Eqs. (10), (11), and (12)],

which could be used to pressures up to 2 kbar. The cell (see Refs. 3, 5, and 17 for more detail) consists essentially of a thin-walled pressure vessel, which allowed us to continuously monitor the hydrogen pressure by means of strain gauges attached to the wall.

Great effort was taken to obtain a long-term stability of the pressure measurement because we had to detect a change of pressure of 5 bars with reasonable accuracy ( $\pm 1$  bar) while our sample was at a pressure 1 kbar for a period of some days. The use of a high-ac excitation voltage (1.5 V) for our resistance strain gauge system enabled short-term detection of pressure changes of  $10^{-2}$  bar. However ohmic heating, in combination with varying heat exchange conditions as the level of our cryogenic fluid (helium) changed, gave a very poor long-term stability. Short-term sensitivity was sacrificed for long-term stability, which was achieved by using a much smaller excitation voltage. We also made optical measurements in a Raman scattering cell<sup>18,19</sup> for the same densities as for the isochoric EOS measurements. For these measurements, light from an argon ion laser (Spectra Physics 165, output typically 1 W at 514.5 nm) was focused through a sapphire window on the hydrogen sample. Light scattered under 90° could be collected and focused on the entrance slit of a double monochromator (Spex 1401). Strain gauges attached on the Raman cell wall allowed crude pressure determination. The cell and more details concerning the concentration  $C_1$  determination by Raman intensity measurements are described in Ref. 18.

In both types of experiments ultra-high-purity hydrogen (Matheson) with a maximum pressure of 2 kbar was introduced into the cells through a  $1 \times 0.16$ -mm stainless steel capillary. The temperature was then lowered until the sample solidified. The freezing point was detected by monitoring the cell pressure (with the strain gauges) and the temperature of the cell. With the known EOS of hydrogen (see Ref. 13) it was possible to determine the density of the sample. Once frozen, the sample remained essentially under isochoric conditions. For the thin-wall isochore cell a small correction was made for the volume change with pressure. The concentration  $C_1$  could not be determined directly in the isochore cell. Instead we start-

ed with  $n\text{-H}_2$  ( $C_1=0.75$ ) and measured the concentration at the end of each run by recovering the sample in a glass cell suitable for analyses by Raman scattering. The conversion rate determined in this way was essentially the same as in that determined in the Raman high-pressure cell (for more details see Ref. 3).

#### IV. EXPERIMENTAL RESULTS

The pressure  $P_{IL}$  [see Eq. (12)] cannot be determined by a direct measurement, as the other contributions to the total pressure are much greater. Only through careful study of the temperature and volume dependence of the total pressure was a separation possible. The pressure  $P_Q$  due to the electric quadrupole moment of the  $J=1$  species, is particularly dependent on  $C_1$  and difficult to separate from  $P_{IL}$ . Fortunately it turns out that the calculated values for  $P_Q$ , Eq. (13), give an adequate description for all measured densities.

Our method of handling the experimental results is illustrated in Figs. 3(a)–3(d). Figure 3(a) shows two isochores for the same molar volumes, but at the extreme values of ortho concentration,  $C_1$ . Our objective is to determine  $P_{IL}(T, V, C_1) = P_{IL} + P_{IL}^*$ , the pressure due to the ortho dependence of the isotropic potential, whereas the quadrupolar pressure,  $P_Q$ , due to the anisotropic interactions we assume to be calculable. For  $C_1=0$  the quadrupolar pressure is zero and we use this as the refer-

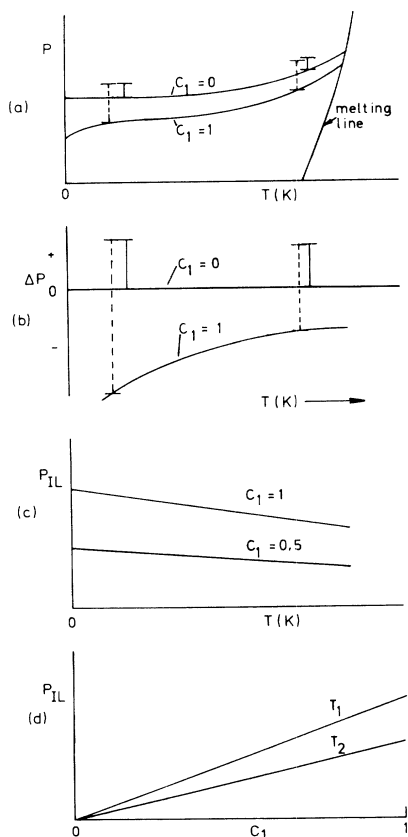


FIG. 3. Schematic picture indicating the method of handling the data. For explanation see text.

ence curve to determine  $P_{IL}$ . The calculated pressure  $P_Q$  for  $C_1=1$  is shown at two temperatures by vertical dashed lines; the solid vertical lines represent the additional increment  $P_{IL}$  required to recover the  $C_1=0$  isochore from the  $C_1=1$  curve. Thus  $P_{IL}$  is determined by inference since the difference between the two curves must be  $\Delta P = P_Q + P_{IL}$ . In Fig. 3(b),  $\Delta P_0$ , the difference between the two curves is plotted, to amplify the effect of interest in the presentation. In Fig. 3(c),  $P_Q$  is subtracted from  $\Delta P$  which leaves  $P_{IL}$  as a function of temperature, shown now for two values of  $C_1$ , relative to  $C_1=0$ . From a series of such measurements,  $P_{IL}$  can be determined as a function of  $C_1$  at constant  $T$  as shown in Fig. 3(d).

We have studied three isochores, which starting from  $C_1=0.75$ , slowly converted to approximately  $C_1=0.2$  (runs 1, 2, and 3). In the literature we found such an experimental run (by Jarvis *et al.*<sup>4</sup>) at nearly zero pressure, which we use as an extra data input (run 0). During our measurements we saw some irregularities in our data. Therefore we included some optical measurements, to study  $C_1$  as a function of time (runs 4, 5, and 6).

##### A. Run 0

Jarvis *et al.*<sup>4</sup> have studied the isochoric variation of pressure at molar volumes of approximately  $22.7 \text{ cm}^3/\text{mole}$ , corresponding to an average pressure of about 40 bars. After subtracting  $P_Q$  for their data we get the results shown in Fig. 4 [which correspond to Fig. 3(d)].

##### B. Run 1

This was our first experimental run. We studied an isochore for nearly one week in order to get a broad range for  $C_1$  (from  $C_1=0.75$  to 0.184). However, the results below  $C_1=0.42$  were unreliable and are not shown here. There were changes in pressure, which were not due to instrumental error or irregularities in the conversion constant  $k$  as a function of time. In run 6, which was done at nearly the same molar volume in the optical Raman scattering cell, we did not observe any unexpected change in  $C_1$ .

Our conclusion is that at some time at the highest temperature during the measurements we had some mass flow out of the capillary so that the molar volume changed. At

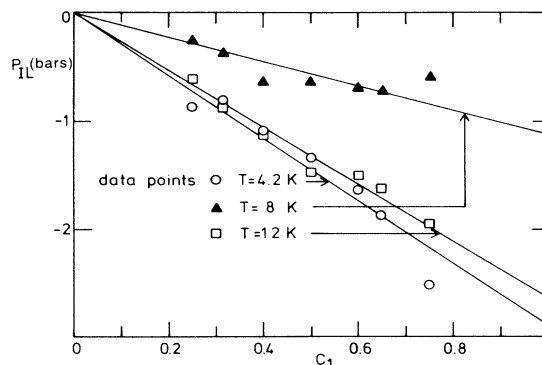


FIG. 4.  $P_{IL}$  as a function of  $C_1$ , run 0,  $V=22.7 \text{ cm}^3/\text{mole}$ .

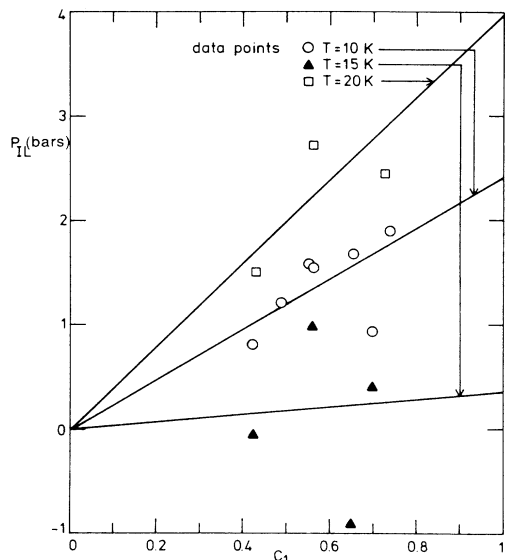


FIG. 5.  $P_{IL}$  as a function of  $C_1$ , run 1,  $V=20.4$  cm<sup>3</sup>/mole.

the end of the run we melted the sample by accident for a short period which resulted in a pressure change of about 100 bar. Therefore we use our data points only in the region before the first irregular step at about  $C_1=0.40$

Figure 5 shows the result presented in the manner of Fig. 3(d). From the melting temperature the volume of this run has been determined to be 20.4 cm<sup>3</sup>/mole by use of the tables given in Ref. 13.

### C. Runs 2 and 3

Run 2 and run 3 are done at nearly the same molar volume: 17.7 and 17.65 cm<sup>3</sup>/mole, respectively. There are no irregularities in the data points. Figure 6 and 7 show the results.

In order to show the magnitude of the observed effects, we have displayed the results of run 3 in Figs. 8 and 9 in more detail. Some isochores with different  $C_1$  are drawn

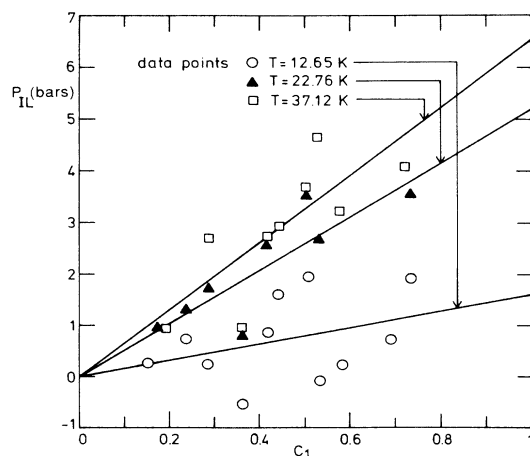


FIG. 6.  $P_{IL}$  as a function of  $C_1$ , run 2,  $V=17.7$  cm<sup>3</sup>/mole.

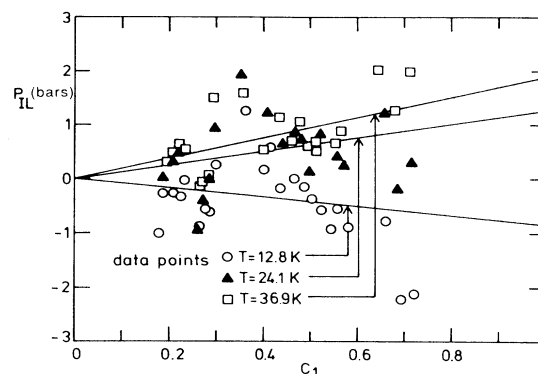


FIG. 7.  $P_{IL}$  as a function of  $C_1$ , run 3,  $V=17.65$  cm<sup>3</sup>/mole.

in Fig. 8 in the form of Fig. 3(a). The analysis of these results in terms of  $P_{IL}(C_1, T)$  and  $P_Q(C_1, T)$  is given in Fig. 9. The dashed lines are the experimental isochores relative to the  $C_1=0$  isochore, or in other words, they represent  $P_{IL}(C_1, T) + P_Q(C_1, T)$  [see also in Fig. 3(b)]. The solid lines give  $P_{IL}(C_1, T)$  as displayed in Fig. 3(c). As can be seen in Fig. 9,  $P_Q$  comes out to be nearly an order of magnitude larger than  $P_{IL}$ . This explains the difficulties in determining the magnitude, or even the sign of  $P_{IL}$ .

### D. Optical runs (4, 5, 6)

In the optical runs, we repeated the isochoric measurements, but now detecting the concentration of  $C_1$  molecules and the phonon frequencies. These runs were done at nearly the same molar volumes as runs 1, 2 and 3. Due to the nature of conversion of ortho to para, in the solid at low temperature the distribution of ortho molecules can become nonrandom.<sup>3</sup> In order to avoid a possible systematic error due to this, the samples were warmed up every 10 h to randomize the distribution. This warming up sometimes resulted in discontinuities in the phonon frequency and also in the concentration  $C_1$ . Equation (15) shows that the change in the rotational quantum

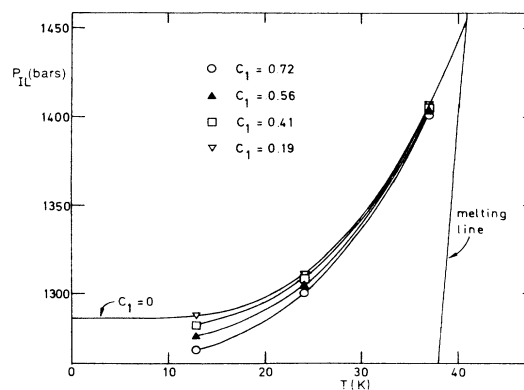


FIG. 8. Some experimental isochores of run 3.

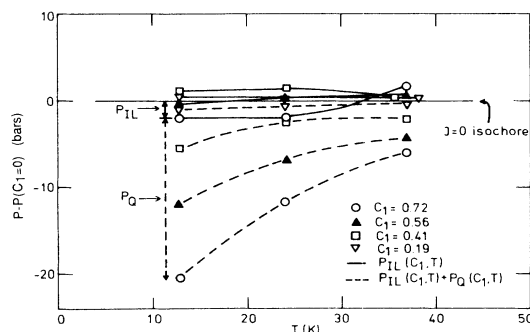


FIG. 9. Analysis of some isochores of run 3 in terms of  $P_Q$  and  $P_{IL}$ . This plot is of the form of Fig. 3(b). As an example,  $P_Q$  and  $P_{IL}$  are shown, the data points indicated by circles.

number of the  $H_2$  molecules will also affect the phonon frequencies. Therefore together with the optical concentration measurements we also determined the frequencies of the Raman active optical phonon. The results are shown in Figs. 10, 11, and 12, with arrows indicating the points of warming up. The straight lines are linear least square fits to the data. The frequency could be determined within  $0.2 \text{ cm}^{-1}$ . The results for the determination of the concentration  $C_1$  are presented and discussed in detail in Ref. 3. In that paper and in the present work, runs I to VI correspond to the same data.

## V. DISCUSSION

Before starting the discussion of the results relevant to  $P_{IL}$ , we can make some conclusions about the calculation of  $P_Q$  with the aid of Eq. (13). The fact that we can reduce a complex temperature, concentration and density dependent pressure effect ( $P_Q + P_{IL}$ ), as we have done in Fig. 9 to a small, weakly temperature dependent effect ( $P_{IL}$ ), gives confidence to the results of our calculations of  $P_Q$ . In our run III at  $17.65 \text{ cm}^3/\text{mole}$  for example,  $P_Q$  ( $C_1=1$ ) is  $-15$  bars at  $37 \text{ K}$ , and  $-33$  bars at  $13 \text{ K}$ , whereas  $P_{IL}$  ( $C_1=1$ ) is small and nearly temperature in-

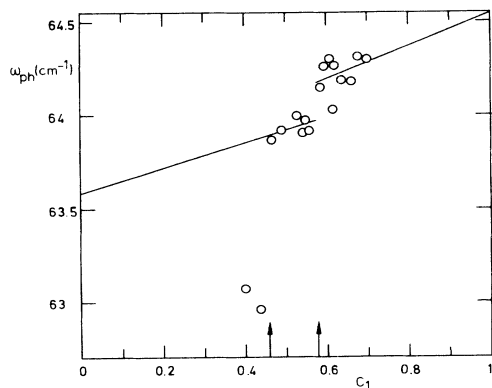


FIG. 10. The frequency of the optical phonon as a function of  $C_1$ ; arrows indicate the points of warming up. Run 4,  $V=18.7 \text{ cm}^3/\text{mole}$ .

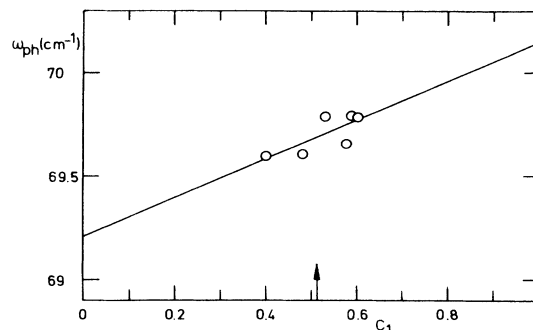


FIG. 11. The frequency of the optical phonon as a function of  $C_1$ ; an arrow indicates the point of warming up. Run 5,  $V=17.6 \text{ cm}^3/\text{mole}$ .

dependent:  $-0.8$  and  $1.9$  bars at these two temperatures.

For  $P_{IL}$ , using the theoretical and experimental results discussed in the preceding sections we find the following picture. When changing from a  $J=0$  state to a  $J=1$  state, the bond length of the molecule changes due to the centripetal force. This has been calculated by Knaap and Beenakker,<sup>6</sup> Eq. (3). The change in bond length results in a change in the isotropic potential which translates into a change in pressure at a certain volume. We have determined this effect at four molar volumes. Due to the subtractive method of data analyses, the experimental error all accumulates on  $P_{IL}$ , giving rise to large scatter because of its small size (Figs. 4–7). The assumption that  $P_{IL}$  depends linearly on  $C_1$  is not inconsistent with the data. Therefore  $P_{IL}$  ( $C_1=1$ ) can easily be deduced from the slope of the straight lines in Figs. 4–7, determined by a least square fit to the experimental points.

Figure 13 shows the experimental  $P_{IL}$  ( $C_1=1$ ) as a function of volume. For all runs we give the result at the same temperatures as in Figs. 4–7. The error bars reflect the number, distribution and quality of the experimental points for  $P_Q + P_{IL}$ , as well as the error in the calculation of  $P_Q$ , which we expect to be proportional to its absolute value. There appears to be a weak temperature dependence due, in part, to error in subtracting other contributions to the total pressure, mainly  $P_Q$ , and in part, to a real temperature dependence of  $P_{IL}$ . This we shall neglect

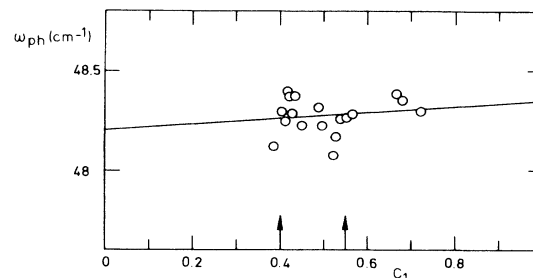


FIG. 12. The frequency of the optical phonon as a function of  $C_1$ ; arrows indicate the points of warming up. Run 6,  $V=20.9 \text{ cm}^3/\text{mole}$ .

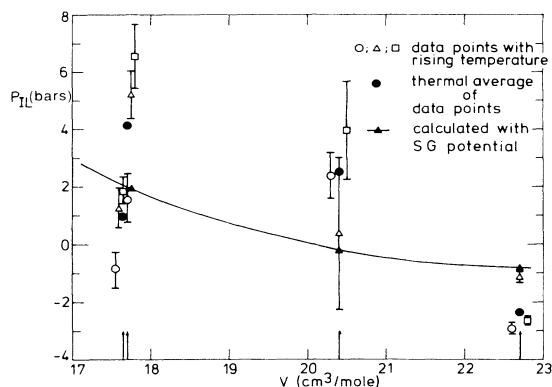


FIG. 13.  $P_{IL}$  as a function of molar volume; arrows indicate the volumes of the four experimental runs. The circle, triangle, and square data symbols represent data at different temperatures, increasing in the order of the symbols shown in the figure legend.

because of the larger errors in determining the contribution of  $P_Q$  to the total pressure.

We would like to give some indication how the experimental  $P_{IL}$  can be interpreted in terms of changes in the parameters of the SG potential, Eqs. (5) and (7) [in the following,  $P_{IL}$  signifies  $P_{IL}(C_2=1)$ ]. We restrict our considerations to the parameters  $C_6$ ,  $C_8$ , and  $C_{10}$  of the multipole expansion of the attractive part and to the leading term in the exponential repulsive part. For these parameters we calculate the partial derivatives of the pressure  $\partial P_{SG}/\partial C_i$  ( $i=6, 8, 10$ ) and  $\partial P_{SG}/\partial \alpha$  by numerical differentiation. We assume

$$P_{IL} = \sum_{i=6,8,10} \frac{\partial P}{\partial C_i} \Delta C_i + \frac{\partial P}{\partial \alpha} \Delta \alpha$$

$$= \sum_{i=6,8,10} P_{ILC_i} + P_{IL\alpha}.$$

$\sum P_{ILC_i}$ , the third column in Table III, can be calculated using the  $\Delta C_i$ 's as given in Table I.

In Table III we give our experimental results  $P_{IL\text{ exp}}$  at four densities and compare these with theoretical calculations. In the fourth column,

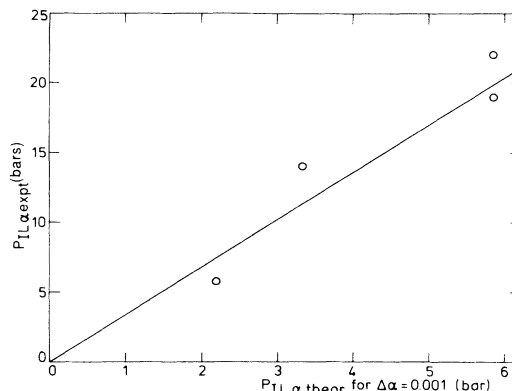


FIG. 14.  $P_{IL\alpha\text{ exp}}$  as a function of  $P_{IL\alpha\text{ theor}}$  for  $\Delta\alpha=0.001$ .

$$P_{IL\alpha\text{ exp}} = P_{IL\text{ exp}} - \sum_{i=6,8,10} P_{ILC_i}$$

is given. In Fig. 14, we plot  $P_{IL\alpha\text{ exp}}$  against  $(\partial P_{SG}/\partial \alpha)\Delta\alpha=0.001$ . We find, within the experimental error bars, a linear relationship

$$P_{IL\alpha\text{ exp}} = 3.4 \times 10^{-3} \frac{\partial P_{SG}}{\partial \alpha}.$$

Our conclusion is therefore that we can describe the effect of changing the bond length with the SG potential by changing the  $C_i$ 's as given in Table I and  $\alpha$  by  $\Delta\alpha=0.0034$ . The resulting  $P_{IL}$  calculated in this way is plotted in Fig. 13 (closed triangles), which compares fairly well with the experimental results averaged over three temperatures (closed circles). The experimentally determined pressure  $P_{IL}$  turns out to be the result of two nearly compensating effects. Due to the larger interatomic distance of the  $J=1$  molecule its polarizability is enhanced, giving a more attractive contribution  $\sum_i P_{ILC_i}$ . On the other hand, the molecule is slightly larger, resulting in a larger hard-core radius and consequently in a larger repulsive contribution  $P_{IL\alpha}$ . At high density (at small intermolecular distance) the repulsive part of the potential will have increasing influence on the resulting pressure. The change of sign of  $P_{IL}$  from a negative pressure at low density to a positive one at higher density confirms

TABLE III. Various theoretically and experimentally determined contributions to the total pressure for runs 0, 1, 2, and 3.

Volume (cm <sup>3</sup> /mole)	$P_{IL\text{ exp}}$ (bars)	$\sum_{i=6,8,10} P_{ILC_i}$ (bars)	$P_{IL\alpha\text{ exp}}$ (bars)	$P_{IL\alpha\text{ theor}}$ $\Delta\alpha=0.0034$ (bars)	$P_{ILSG}$ (bars)
22.7	-2.4	-8.2	5.8	7.4	-0.8
20.4	2.5	-11.5	14.0	11.3	-0.2
17.7	4.1	-18.0	22.1	19.9	1.9
17.65	1.0	-18.0	19.0	19.9	1.9

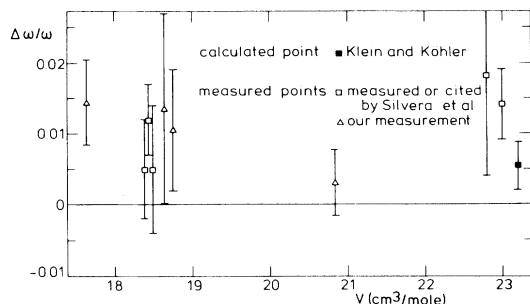


FIG. 15. The shift  $\Delta\omega_{\text{tot}}/\omega$  in the frequency of the optical phonon as a function of molar volume.

this qualitative picture.

Besides an effect on the potential, the changed bond length will have an influence on the phonon frequency at constant volume. Figure 15 shows the relative change in frequency as function of density. Together with our experimental points (triangles) which are in the slope of the straight lines in Figs. 10–12, determined by a least square fit to the experimental points, we give data points of Silvera *et al.*<sup>20</sup> and Jochemsen<sup>21</sup> as redetermined in Ref. 20. Our measurements are in good agreement with theirs.

We also include the calculated frequency shift at zero pressure by Klein and Koehler<sup>22</sup> (closed square). In Eq. (15) we gave the different contributions to the shift in the phonon frequency due to the change in rotational state of the  $\text{H}_2$  molecules. There are two main contributions to  $\Delta\omega_{\text{tot}}$ : a direct one,  $\omega_{IL}$ , and an indirect one caused by changes in pressure at constant volume when going from  $C_1=0$  to  $C_1=1$ :  $(\Delta\omega_{\text{tot}}/\Delta P)(P_Q + P_{IL})$ . The calculation of Klein and Koehler<sup>22</sup> gives only a value for  $\omega_{IL}$ .

We can make an estimate for the indirect term. The sum of  $P_Q$  and  $P_{IL}$ , which we have determined in Eq. (13) and in Fig. 13, can amount to 30% of the pressure change on an isochore in the solid. Silvera *et al.*<sup>20</sup> have measured the frequency of the phonon as a function of temperature on an isochore at  $18.45 \text{ cm}^3/\text{mole}$ . They find for the whole trajectory up to the melting line  $\Delta\omega/\omega \sim 5\%$ . As shown in Eq. (15), the phonon frequency change has a temperature-dependent and -independent part. If we assume that the temperature-induced pressure change along the isochore is mainly responsible for  $\Delta\omega$ , we estimate the indirect term to be 30% of 5%, or 1.5%. For one molar volume,  $V=18.45$  we can give a more detailed analysis. Silvera *et al.*<sup>20</sup> have measured for this volume  $\Delta\omega_{\text{tot}}$  at 5, 15, and 25 K. When we analyze their data as plotted in their Fig. 6, we get  $(\Delta\omega_{\text{tot}}/\omega)/\Delta P \sim 3.4 \times 10^{-4}/\text{bars}$ . We can calculate  $P_Q$  and  $P_{IL}$  as a function of temperature

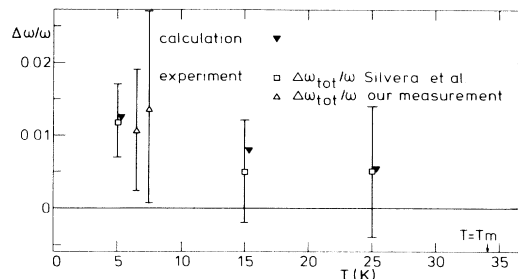


FIG. 16. The shift  $\Delta\omega_{\text{tot}}/\omega$  in the frequency of the optical phonon as a function of temperature  $V \sim 18.45 \text{ cm}^3/\text{mole}$ . The calculated points (triangles) are estimates for the indirect contribution in Eq. (15).

from Eq. (13) and Fig. 13. We expect the neglect of  $\Delta\omega_Q$  to be a good approximation. In this way we are able to determine the indirect term. Figure 16 shows the different contributions to the frequency shift for one molar volume,  $V=18.45 \text{ cm}^3/\text{mole}$ . We also include our own data at slightly different molar volumes ( $V=17.65$  and  $17.7 \text{ cm}^3/\text{mole}$ ). As can be seen the indirect term alone can explain the frequency shift. Our conclusion is that  $\omega_{IL}/\omega$  is small, probably less than 1%.

## VI. SUMMARY

In this paper we have studied the influence of the rotational state of  $\text{H}_2$  on the pair interaction potential, the EOS and the frequency of the optical phonon. Analysis of the EOS data confirmed that the expression for  $P_Q$ , Eq. (13), which was based on heat-capacity data at zero pressure, is also valid at higher pressures (at least up to 2 kbar). On the basis of *a priori* calculations and experimental data, the change of rotational state can be expressed in terms of the parameters of the SG potential. The calculations of  $P_{IL}$  on the basis of this set of parameters are at least in qualitative agreement with the experiment. The measured shift in phonon frequency at constant volume,  $\Delta\omega_{\text{tot}}/\omega$ , is induced to a great extent by the pressure  $P_Q + P_{IL}$ . The direct contribution,  $\omega_{IL}$ , is expected to be less than 1%.

## ACKNOWLEDGMENTS

We would like to thank V. V. Goldman for stimulating discussions, and E. van der Poll for assistance during the experiments. The Stichting Fundamental Onderzoek der Materie (FOM) and the National Science Foundation, Grant No. DMR-8600955 are acknowledged for support.

\*Present address: Natuurkundig Laboratorium, Vrije Universiteit, Amsterdam, The Netherlands.

<sup>1</sup>J. Van Kranendonk, *Solid Hydrogen* (Plenum, New York, 1983).

<sup>2</sup>I. F. Silvera, *Rev. Mod. Phys.* **52**, 393 (1980), and references given therein.

<sup>3</sup>A. Driessen, E. van der Poll, and I. F. Silvera, *Phys. Rev. B* **30**,

2517 (1984).

<sup>4</sup>J. F. Jarvis, H. Meyer, D. Ramm, *Phys. Rev.* **178**, 1461 (1969).

<sup>5</sup>A. Driessen, J. A. de Waal, and I. F. Silvera, *J. Low Temp. Phys.* **34**, 225 (1979).

<sup>6</sup>H. F. P. Knaap and J. J. M. Beenakker, *Physica* **27**, 523 (1961).

<sup>7</sup>I. F. Silvera and V. V. Goldman, *J. Chem. Phys.* **69**, 4209 (1978).

- <sup>8</sup>W. Meyer, *Chem. Phys.* **17**, 27 (1976).
- <sup>9</sup>A. K. McMahan, H. Beck, and J. A. Krumhansl, *Phys. Rev. A* **9**, 1852 (1974).
- <sup>10</sup>F. H. Ree and C. F. Bender, *J. Chem. Phys.* **71**, 5362 (1979).
- <sup>11</sup>B. I. Min, H. J. F. Jansen, and A. J. Freeman, *Phys. Rev. B* **33**, 6383 (1986).
- <sup>12</sup>W. Kolos and L. Wolniewicz, *J. Chem. Phys.* **41**, 3674 (1964).
- <sup>13</sup>A. Driessen and I. F. Silvera, *J. Low Temp. Phys.* **54**, 361 (1984).
- <sup>14</sup>A. J. Berlinsky and A. B. Harris, *Phys. Rev. A* **1**, 878 (1970).
- <sup>15</sup>We thank Dr. L. A. Schwalbe for pointing out a discrepancy between the numerical results in the table and experimental results. The error in the tabulation was due to a constant numerical unit-conversion error.
- <sup>16</sup>We thank Dr. V. V. Goldman for making these codes available to us.
- <sup>17</sup>A. Driessen, Ph.D. thesis, University of Amsterdam, 1982.
- <sup>18</sup>P. J. Berkhout, Ph.D. thesis, University of Amsterdam, 1978.
- <sup>19</sup>P. J. Berkhout and I. F. Silvera, *J. Low Temp. Phys.* **36**, 231 (1979).
- <sup>20</sup>I. F. Silvera, P. J. Berkhout, and L. M. van Aernsbergen, *J. Low Temp. Phys.* **35**, 611 (1979).
- <sup>21</sup>R. Jochemsen, Ph.D. thesis, University of Amsterdam, 1978.
- <sup>22</sup>M. L. Klein and T. R. Koehler, *J. Phys. C* **3**, L102 (1970).